Letter

Strongly enhanced nonlinear acoustic valley Hall effect in tilted Dirac materials

Jia-Liang Wan, Ying-Li Wu, Ke-Qiu Chen, and Xiao-Qin Yu*

School of Physics and Electronics, Hunan University, Changsha 410082, China

(Received 18 November 2023; revised 27 February 2024; accepted 1 March 2024; published 1 April 2024)

It has been recently established that a nonlinear valley current can be generated through propagating a surface acoustic wave (SAW) in two-dimensional Dirac materials. So far, the SAW-driven valley currents have been attributed to the warped Fermi surface or the Berry phase effect. Here, we demonstrate that the tilt mechanism can also lead to a nonlinear valley Hall current (VHC) when propagating SAWs in materials with the tilted Dirac cone placed on a piezoelectric substrate. It has been found that the nonlinear VHC exhibits a $\sin\theta$ dependence on the orientation of the tilt with respect to the SAW. In addition, this tilt-induced nonlinear acoustic VHC shows independence of the relaxation time, distinguished from the contributions from the Berry phase or trigonal warping. Remarkably, the magnitude of the nonlinear acoustic VHC from the tilt mechanism in the uniaxially strained graphene is 2 orders larger than those reported in MoS_2 stemming from the Berry phase effect and the warping effect.

DOI: 10.1103/PhysRevB.109.L161101

Introduction. The valley, an extra degree of freedom of electron, in two-dimensional (2D) crystal with honeycomb lattice structure shows the potential to store and carry information instead of electron and spin, leading to the emergence of valleytronics [1–5], in which the generation of a valley current is a vital issue. The major approaches, nowadays, to generate a valley current are through the valley Hall (Nernst) effect [1,6], which indicates electrons with different valleys (K and −K valleys) flowing in the opposite direction perpendicular to an applied electric field (temperature gradient) without breaking time-reversal symmetry. The generated valley current shows a linear dependence on the driven forces and can be attributed to a nonvanishing Berry curvature [7,8] of all occupied energy bands.

Recently, the nonlinear anomalous Hall effect [9–16] in time-reversal-invariant noncentrosymmetric materials as a second-order response to an electric field, which stems from the dipole moment of Berry curvature near the Fermi level (namely, Berry curvature dipole) [9–15], has attracted broad interest in the study of other nonlinear anomalous transport phenomena, such as the nonlinear spin Hall effect [17,18], the nonlinear thermal Hall effect [19,20], and the nonlinear anomalous Nernst effect [21–23]. All those effects are related to a geometric property of electron wave functions, namely, Berry curvature near the Fermi level, and driven by an electric field or temperature gradient.

In addition to the electron flows driven by an electric field and the temperature gradient, acoustic waves can, actually, also drive carriers and generate an electric current through interaction with electrons. The acoustoelectric effect (AEE) [24,25], referring to a generation of electric current in response to the traveling acoustic wave, was first theoretically proposed by Parmenter [24] in 1953 and observed in experiment by Weinreich and White in 1957 [25]. The standard AEE originates in the sound-induced strain field and the corresponding deformation potential which perturbs and drags electrons resulting in an electric current along the acoustic wave vector. Apart from the deformation potential mechanism, a piezoelectric mechanism of interaction between surface acoustic waves (SAWs) and electrons has also been explored in low-dimensional systems (LDS) [26–30]. When placing the LDS on the piezoelectric substrate, the Bleustein-Gulyaev acoustic wave generated through the interdigital transducers [Fig. 1(a)] will induce a piezoelectric field and distort the ionic lattice, resulting in a local imbalance of the electric chemical potential μ and leading to density fluctuation and nonequilibrium electron distribution. Consequently, the induced piezoelectric field drags carriers and gives rise to electron current.

Owing to the appearance of new 2D materials, the studies of SAWs are stimulated. The interactions with electrons have been investigated in monolayer graphene [31,32], the surface of the topological insulators [33]. A few new acoustoelectric responses have been recently predicted, including the acoustic drag effect [34], the valley acoustoelectric effect in two-dimensional transition metal dichalcogenides (TMDs), and the pseudoelectromagnetic-field-induced acoustogalvanic effect in Dirac and Weyl materials [35–37]. Among them, a nonlinear acoustoelectric valley Hall effect (AVHE) as a second-order response to the SAW-induced field stemming from piezoelectric or deformation potential mechanisms has been reported in TMDs placed on a piezoelectric substrate [38] or a nonpiezoelectric substrate [39], respectively. For the deformation potential mechanism [39], the warped Fermi surface is crucial to get a nonvanishing AVHE. In the piezoelectric case [38], in addition to the warping effect of the Fermi surface, the nontrival Berry phase can also give rise to the AVHE.

In this Letter, we report a contribution to the nonlinear AVHE: the tilting effect of Dirac cones. We show that the nonlinear AVHE does emerge even in the complete absence

*yuxiaoqin@hnu.edu.cn

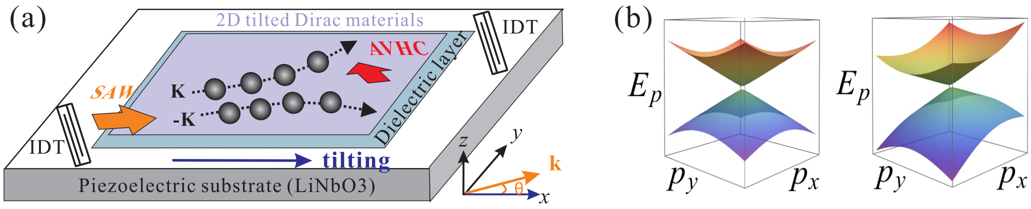

FIG. 1. (a) Illustration of the generation of the VAHE through SAW for a tilted mechanism in a 2D material placed on a piezoelectric substrate. θ is the azimuthal angle of the surface acoustic wave vector $\mathbf{k}$ with respect to the tilting direction (x direction). (b) The band structure of the two-dimensional Dirac materials with (right) or without (left) tilting in the p_x direction.

of warping electron dispersion and without considering the Berry phase in the 2D titled Dirac system.

Acoustoelectric effect in 2D Dirac material. The formulas for nonlinear current generated from the SAW via the AEE have been recently determined through the semiclassical framework of electron dynamics [38]. We start by recalling the formulas. When propagating a Bleustein-Gulyaev SAW with wave vector $\mathbf{k}$ and frequency ω along the interface of the 2D materials and the piezoelectric substrate, an in-plane piezoelectric field $\mathbf{E}(\mathbf{r},t) = \mathrm{Re}(\mathbf{E}e^{i\mathbf{k}\cdot\mathbf{r}-i\omega t})$ will be created. Meanwhile, an induced electric field $\mathbf{E}^i(\mathbf{r},t)$ stemming from the fluctuations of the electron density will also emerge owing to the perturbation of the SAW, which can be determined through Maxwell's equations (see details in Ref. [40]). Subsequently, the overall electric field $\widetilde{\mathbf{E}}(\mathbf{r},t)$, which includes the in-plane piezoelectric field $\mathbf{E}(\mathbf{r},t)$ and the induced electric field $\mathbf{E}^i(\mathbf{r},t)$, will drag the carriers in 2D materials, giving rise to a nonlinear current. The nonlinear current in response to the SAW-induced electric field can be formally decomposed into drift and diffusive components $j_a = j_a^{\mathrm{dr}} + j_a^{\mathrm{di}}$, with $j_a^{\mathrm{dr}} = \mathrm{Re}(\chi_{abc}^{\mathrm{dr}}\widetilde{E}_b^*\widetilde{E}_c)$ and $j_a^{\mathrm{di}} = \mathrm{Re}(\chi_{abc}^{\mathrm{di}}\widetilde{E}_b^*\widetilde{E}_c)$ (the superscripts "dr" and "di" refer to drift and diffusive, respectively). The response functions χ_{abc}^{dr} and χ_{abc}^{di} have the forms

$$\chi_{abc}^{\mathrm{dr}} = -2e^3\tau^2 Q_{abc},$$
$$\chi_{abc}^{\mathrm{di}} = -2e\tau\frac{\partial\mu}{\partial n}P_{ab}k_d\sigma_{dc}/(\omega - \mathbf{k}\cdot\mathbf{R}), \quad (1)$$

where $a, b, c, d \in \{x, y\}$; τ represents the scattering time; μ refers to the chemical potential; n denotes the electron density; $\mathbf{R}$ and σ_{dc} indicate the diffusion vector and the conductivity tensor, respectively, the formulas of which are given in Ref. [40]; and the pseudotensorial quantities Q_{abc} and P_{ab} are defined, respectively, as

$$Q_{abc} = \frac{1}{2\hbar}\int\frac{d\mathbf{p}}{(2\pi)^2}\frac{\partial v_a}{\partial p_b}\frac{v_c}{1 - i(\omega - \mathbf{k}\cdot\mathbf{v})\tau}\left(-\frac{\partial f(\varepsilon_{\mathbf{p}})}{\partial\varepsilon_{\mathbf{p}}}\right) \quad (2)$$

$$P_{ab} = \frac{1}{2\hbar}\int\frac{d\mathbf{p}}{(2\pi)^2}\frac{\partial v_a}{\partial p_b}\frac{1}{1 - i(\omega - \mathbf{k}\cdot\mathbf{v})\tau}\left(-\frac{\partial f(\varepsilon_{\mathbf{p}})}{\partial\varepsilon_{\mathbf{p}}}\right), \quad (3)$$

where ħ is the Planck constant, $\varepsilon_{\mathbf{p}}$ is the energy of the electron with momentum $\mathbf{p}$, $\mathbf{v} = \partial\varepsilon_{\mathbf{p}}/\hbar\partial\mathbf{p}$ is the velocity of electron, and $f(\varepsilon_{\mathbf{p}})$ indicates the equilibrium Fermi-Dirac distribution function in the absence of the perturbation of the SAW.

Model. the effective Hamiltonian of tilted Dirac systems is

$$H_d = v_F\hbar(\eta p_x\sigma_x + p_y\sigma_y) + \sigma_z\Delta/2 + \eta t p_x, \quad (4)$$

where $\hat{\boldsymbol{\sigma}}$ denotes the Pauli matrices for the two basis functions of energy bands, $\eta = \pm 1$ indicates the valley index, Δ presents the energy gap, and t is the tilting parameter. For simplicity, we only focus on the n-doped system, and the energy eigenvalue of the conduction band is

$$\varepsilon_{\mathbf{p}} = \sqrt{\left(\frac{\Delta}{2}\right)^2 + (v_F\hbar p)^2} + \varepsilon_t, \quad (5)$$

where $\varepsilon_t = \eta t p_x$ is the tilt-induced energy shift. The band structures with and without the tilting effect are illustrated in Fig. 1(b). The partial derivative of the Fermi-Dirac distribution $f(\varepsilon_{\mathbf{p}})$ function with respect to the energy $\varepsilon_{\mathbf{p}}$ in Eqs. (2) and (3) to the first order of the tilting effect can be written as

$$\frac{\partial f(\varepsilon_{\mathbf{p}})}{\partial\varepsilon_{\mathbf{p}}} = \frac{\partial f_0}{\partial\varepsilon_{\mathbf{p}}^0} + \varepsilon_t\frac{\partial^2 f_0}{\partial\left(\varepsilon_{\mathbf{p}}^0\right)^2}, \quad (6)$$

where $\varepsilon_{\mathbf{p}}^0 = \sqrt{(\frac{\Delta}{2})^2 + (v_F\hbar p)^2}$ is the energy without the tilting effect. Combining Eqs. (1), (2), and (3) with Eqs. (5) and (6), the total nonlinear current can determined and would be decomposed into two parts as $\mathbf{j}^{\mathrm{total}} = \sum_\eta \mathbf{j}_\eta^{\mathrm{tilt}} + \mathbf{j}_{\mathrm{c}}^{\mathrm{di}}$ corresponding to the tilt-induced valley-dependent current $\mathbf{j}_\eta^{\mathrm{tilt}}$ and the conventional diffusive current $\mathbf{j}_{\mathrm{c}}^{\mathrm{di}}$ with the subscript "c" (superscript "di") referring to conventional (diffusive), respectively [40]. The conventional diffusive current $\mathbf{j}_{\mathrm{c}}^{\mathrm{di}}$ is found to be collinear with SAW and does not depend on the valley index and the tilting effect, having no contribution to the valley Hall current [40]. Thus, we ignore this conventional diffusive current when studying the nonlinear acoustic valley Hall effect in the following.

When propagating the SAW along the $\vec{e}_{\mathbf{k}} = (\cos\theta, \sin\theta)$ direction, where the azimuth angle θ is measured from the tilting direction (x direction), the tilt-induced valley-dependent currents $\mathbf{j}_\eta^{\mathrm{tilt}}$ for the η valley in the x and y directions as the response to the SAW-induced field are found to be [40], respectively,

$$\begin{pmatrix} j_{\eta,x}^{\mathrm{tilt}} \\ j_{\eta,y}^{\mathrm{tilt}} \end{pmatrix} = \eta\Upsilon_{\mathrm{A}}^{\mathrm{tilt}}\begin{pmatrix} 2 + \cos 2\theta \\ \sin 2\theta \end{pmatrix}E_0^2, \quad (7)$$

where $E_0 = k\varphi_{\mathrm{SAW}}$ is the piezoelectric field amplitude linearly dependent on the magnitude of the SAW wave vector k and the acoustic wave piezoelectric potential amplitude φ_{SAW}, and the valley-independent nonlinear current response function (NCRF) amplitude $\Upsilon_{\mathrm{A}}^{\mathrm{tilt}} = \Upsilon_{\mathrm{A}}^{\mathrm{dr}} + \Upsilon_{\mathrm{A}}^{\mathrm{di}}$ (the subscript "A" represents the amplitude) is the sum of the tilt-induced drift NCRF amplitude $\Upsilon_{\mathrm{A}}^{\mathrm{dr}}$ and the tilt-induced diffusive NCRF amplitude

$\Upsilon_{\mathrm{A}}^{\mathrm{di}}$, which are given by, respectively,

$$\Upsilon_{\mathrm{A}}^{\mathrm{dr}} = -\frac{te^3\tau^2}{16\pi\hbar^3}\gamma_0\frac{1+(\sigma/\sigma_*)^2(ak\varepsilon_1/E_f)^2}{1+(\sigma/\sigma_*)^2(1+ak\varepsilon_1/E_f)^2},$$
$$\Upsilon_{\mathrm{A}}^{\mathrm{di}} = \frac{te^3\tau^2}{16\pi\hbar^3}\gamma_0\frac{(\sigma/\sigma_*)^2(ak\varepsilon_1/E_f)^2}{1+(\sigma/\sigma_*)^2(1+ak\varepsilon_1/E_f)^2}, \quad (8)$$

leading to

$$\Upsilon_{\mathrm{A}}^{\mathrm{tilt}} = -\frac{te^3\tau^2}{16\pi\hbar^3}\gamma_0\frac{1}{1+\gamma(E_f,\tau)}, \quad (9)$$

where the auxiliary function $\gamma_0 = 1+2\varsigma^2-3\varsigma^4$ is determined through $\varsigma = \Delta/2E_f$, $\gamma(E_f,\tau) = (\sigma/\sigma_*)^2(1+ak\varepsilon_1/E_f)^2$, with $\varepsilon_1 = m_e v_F^2/2$, two defined parameters $\sigma_* = \epsilon_0(\epsilon+1)v_s/4\pi$ and $a = \epsilon_0(\epsilon+1)\hbar^2/(2m_e e^2)$ are dependent on the dielectric permittivity of vacuum ϵ_0 and the dielectric constant ϵ of substrate with the sound velocity v_s [39] and the free electron mass m_e, and $\sigma = e^2\tau E_f(1-\varsigma^2)/2\pi\hbar^2$ denotes the static conductivity of the system. The formula of the tilt-induced NCRF amplitude $\Upsilon_{\mathrm{A}}^{\mathrm{tilt}}$ in Eq. (9) can be further simplified in the following two limits of γ as

$$\Upsilon_{\mathrm{A}}^{\mathrm{tilt}} \approx \begin{cases} -\frac{t\pi\hbar}{e\Delta^2}\frac{\varsigma^2(1+3\varsigma^2)}{(1-\varsigma^2)(1+ak\varepsilon_1/E_f)^2}\sigma_*^2, & \gamma(E_f,\tau)\gg 1,\\ -\frac{te^3\tau^2}{16\pi\hbar^3}\gamma_0, & \gamma(E_f,\tau)\ll 1,\end{cases} \quad (10)$$

showing the following relaxation-time dependence: $\Upsilon_{\mathrm{A}}^{\mathrm{tilt}} \propto \tau^2$ when $\gamma(E_f,\tau)\ll 1$ and $\Upsilon_{\mathrm{A}}^{\mathrm{tilt}} \propto \tau^0$ when $\gamma(E_f,\tau)\gg 1$. It should be pointed out that $\gamma(E_f,\tau)\ll 1$ corresponds to the highly disordered and low-doped systems, whereas $\gamma(E_f,\tau)\gg 1$ can be valid if one does not consider the highly disordered and low-doped systems [38]. Based on the relaxation-time independence in the regime where $\gamma(E_f,\tau)\gg 1$, the tilting contribution to the acoustic valley Hall effect can be easily distinguished from the Berry phase or trigonal warping [38], since the Berry-phase-induced acoustic valley Hall current (AVHC) has been found to be inversely proportional to relaxation time τ and the AVHC from the trigonal-warping contribution has $A+B\tau^2$ dependence on the relaxation time τ. Therefore, one could separate the tilt-induced AVHC from the Berry-phase-induced one through the scaling relations $j^{\mathrm{tilt}} \propto \rho_{xx}^0$ and $j^{\mathrm{Bp}} \propto \rho_{xx}$, where the superscripts "Bp" represents the Berry phase and ρ_{xx} denotes the longitudinal resistivity.

According to Eq. (7), one can observe that although the total tilt-induced nonlinear current $\mathbf{j}_{\mathrm{total}}^{\mathrm{tilt}} = \mathbf{j}_{\eta=+1}^{\mathrm{tilt}} + \mathbf{j}_{\eta=-1}^{\mathrm{tilt}}$ summed over the valley indices η is vanishing due to the time-reversal symmetry, the valley current $\mathbf{j}_{\mathrm{valley}}^{\mathrm{tilt}} = \mathbf{j}_{\eta=+1}^{\mathrm{tilt}} - \mathbf{j}_{\eta=-1}^{\mathrm{tilt}}$ stemming from the tilting effect is nonzero. Equation (7) also hints that when the SAW is parallel or antiparallel to the tilting direction (i.e., $\theta = 0, \pi,$), namely, in the x direction, the valley current manifests itself as a longitudinal current in response to the SAW and there is no valley Hall current flowing vertically to the SAW since only the x component of $\mathbf{j}_{\mathrm{valley}}^{\mathrm{tilt}}$, which is aligned to the SAW, is nonzero. When the SAW propagates perpendicularly to the tilting direction (i.e., $\theta = \pi/2, 3\pi/2$), the valley current still only has a nonzero component in the x direction but behaves as a valley transverse current (i.e., valley Hall current) since the current, actually, flows vertically to the SAW in this situation.

Actually, the angular dependence of the nonlinear longitudinal current $j_{\eta,\parallel}^{\mathrm{tilt}}$ collinear with the SAW and the transverse current $j_{\eta,\perp}^{\mathrm{tilt}}$ vertically to the SAW for the valley η as the second-order response to the SAW-induced field are found to be, respectively [40],

$$j_{\eta,\parallel}^{\mathrm{tilt}} = \cos\theta\, j_{\eta,x}^{\mathrm{tilt}} + \sin\theta\, j_{\eta,y}^{\mathrm{tilt}} = 3\eta\cos\theta\,\Upsilon_{\mathrm{A}}^{\mathrm{tilt}}E_0^2,$$
$$j_{\eta,\perp}^{\mathrm{tilt}} = -\sin\theta\, j_{\eta,x}^{\mathrm{tilt}} + \cos\theta\, j_{\eta,y}^{\mathrm{tilt}} = -\eta\sin\theta\,\Upsilon_{\mathrm{A}}^{\mathrm{tilt}}E_0^2, \quad (11)$$

showing that the amplitude of the nonlinear longitudinal current $j_{\eta,\parallel}^{\mathrm{tilt}}$ aligned to the SAW is triple of that of the nonlinear transverse current $j_{\eta,\perp}^{\mathrm{tilt}}$ which flows vertically to the SAW, namely, the nonlinear Hall current. Therefore, the SAW-driven nonlinear AVHC $j_{\mathrm{H}}^{\mathrm{valley}}$ stemming from the tilting effect in the tilted Dirac system is

$$j_{\mathrm{H}}^{\mathrm{valley}} = j_{+1,\perp}^{\mathrm{tilt}} - j_{-1,\perp}^{\mathrm{tilt}} = -2\sin\theta\,\Upsilon_{\mathrm{A}}^{\mathrm{tilt}}E_0^2. \quad (12)$$

Equations (9) and (12) show that $j_{\mathrm{H}}^{\mathrm{valley}}$ exhibits a $\sin\theta$ dependence on the orientation of the SAW with respect to the tilting direction and is proportional the tilting parameter component in the vertical direction to the SAW, namely, $t\sin\theta$. Thus, when the tilt is perpendicular to the SAW (i.e., $\theta = \pi/2, 3\pi/2$), the magnitude of $|j_{\mathrm{H}}^{\mathrm{valley}}|$ will reach its maximum. However, once the tilt is aligned to the direction of the SAW, namely, $\theta = 0$ or π, the acoustic nonlinear valley Hall current $j_{\mathrm{H}}^{\mathrm{valley}}$ vanishes.

The disappearing $j_{\mathrm{H}}^{\mathrm{valley}}$ can be attributed to the mirror reflection symmetry. Essentially, the tilt does not break the mirror reflection symmetry of each valley along the direction vertical to the tilt [Figs. 2(a) and 2(b)]. The survived mirror symmetry requires no nonlinear current flowing perpendicularly to the tilt, meaning no acoustic nonlinear Hall current is generated. To understand the restriction of mirror symmetry on the nonlinear current orthogonal to the mirror plane, let us assume the tilt is along the l direction. Hence, the mirror symmetry $m_{l_\perp}$ is survived. Under the mirror symmetry $m_{l_\perp}$, $v_{l_\perp}$, $p_{l_\perp}$, and $\tilde{E}_{l_\perp}$ change sign while $\varepsilon_{\mathbf{p}}$, p_l, and $\tilde{E}_l$ are invariant, where $l_\perp$ indicates a vector orthogonal to the vector l in the 2D plane. Hence, when the system is invariant under the mirror symmetry $m_{l_\perp}$, the integration of the nonlinear acoustic current $j_{l_\perp} = -\frac{e^2\tau}{\hbar}\mathrm{Re}\int\frac{d\mathbf{p}}{(2\pi)^2}v_{l_\perp}\tilde{\mathbf{E}}\cdot\frac{\partial f_1}{\partial\mathbf{p}}$ in the $l_\perp$ direction for each valley is an odd function with respect to $p_\perp$, hinting that there is no acoustic nonlinear valley current generation vertical to the mirror plane ($j_{l_\perp} = 0$).

One candidate Dirac material to observe the predicted nonlinear AVHE stemming from the tilting effect is the armchair uniaxially strained graphene monolayer. When applying a slight uniaxial strain, u_{yy} ($< 5\%$), along the armchair, the tilting parameter t can be determined by $t = 0.6u_{yy}v_F\hbar$, and meanwhile the strain-induced anisotropy of the Fermi velocity would be rarely taken into account [43–45]. Besides, further depositing a hexagonal boron nitride (h-BN) dielectric layer between the piezoelectric substrate and the graphene [41,46–48], a staggered chemical potential, Δ (Semeoff mass, or energy gap), can be generated and gap values as large as $\Delta \approx 5\sim 40$ meV can be realized [41]. When taking $\Delta = 5$ meV,

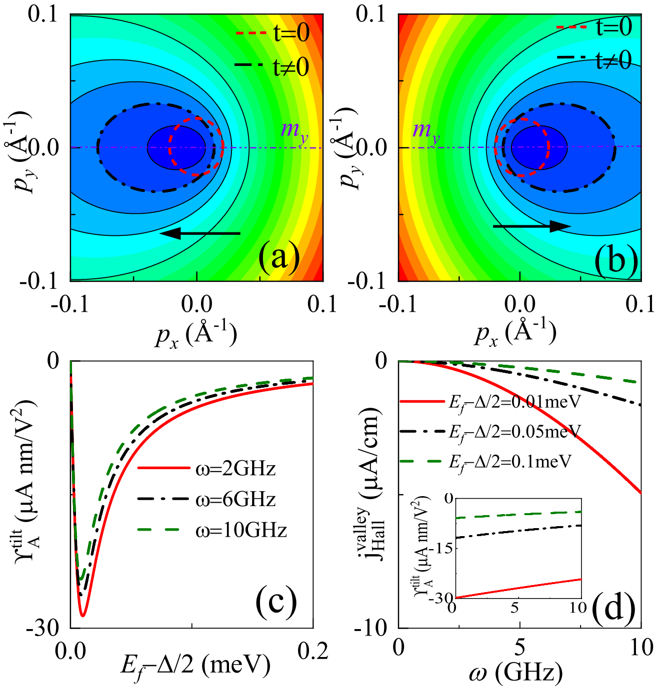

FIG. 2. (a) and (b) Schematic of the energy contour of the K valley [(a)] and the −K valley [(b)] with or without the tilting effect. The contours show that the mirror symmetry m_y is survived when the tilt is along the x direction. (c) Υ_A^{tilt} versus the Fermi energy $E_f - \Delta/2$ at different frequencies ω of the SAW. (d) Dependence of the tilt-induced nonlinear AVHC j_{Hall}^{valley} on the SAW frequency ω. The inset shows the frequency dependence of the Υ_A^{tilt}. The black arrows in panels (a) and (b) represent the tilting direction. Parameters used here are as follows: $\Delta = 5$ meV [41], $v_F = 0.8 \times 10^6$ m/s [42], and $t = 0.03 v_F \hbar$ for the uniaxial strain of order 5%.

the effective mass of electron $m \approx \Delta/(2v_F)^2$ near the Dirac cone is 7×10^{-4} m_e, with m_e presenting the free electron mass [41]. The mobility μ_e of the graphene placed on the h-BN layer ranges from 8×10^4 to 2.75×10^5 cm^2 V^{-1} s^{-1} [48] at low density ($n < 10^{-10}$ cm^{-2}). We take $\mu_e = 2.7 \times 10^5$ cm^2 V^{-1} s^{-1}. Therefore, the scattering relaxation time $\tau = 0.1$ ps is estimated by $\tau = \mu m/e$. To numerically analyze the behaviors of the tilt-induced AVHE in the uniaxial strained graphene, we choose $LiNbO_3$ as the piezoelectric substrate and the corresponding material parameters are taken as follows: the sound velocity $v_s = 3500$ m/s, the dielectric constant $\epsilon = 50$ [49], and the acoustic wave piezoelectric potential amplitude $\varphi_{SAW} = 50$ mV, which determines the amplitude of the piezoelectric field $E_0 = k\varphi_{SAW}$ $(k = \omega/v_s)$.

Figure 2(c) shows the dependence of the tilt-induced NCRF amplitude Υ_A^{tilt} on the Fermi energy E_f with different frequencies. Obviously, the maxima of the tilt-induced NCRF amplitude Υ_A^{tilt} can be obtained by modulating the Fermi energy close to the Dirac point within 0.02 meV through the gate voltage. Therefore, the tilt-induced nonlinear AVHC can be easily separated from the warping effect since the warping effect has a significant contribution to the nonlinear AVHC only when the Fermi energy is far away from the Dirac point. Although the magnitude of the peak value of Υ_A^{tilt} is enhanced with decreasing the frequency [Figs. 2(c) and 2(d)], the tilt-induced AVHC j_H^{valley} increases when enhancing the frequency owing to $j_H^{valley} \sim \Upsilon_A^{tilt}\omega^2$ [Fig. 2(d)]. To estimate the tilt-induced acoustic nonlinear valley Hall effect, we take $\Upsilon_A^{tilt} = 24.2$ μA nm/V^2 at $E_f - \Delta/2 = 0.01$ meV and $\omega = 10$ GHz. Hence, the pure AVHC $j_H^{valley} = \Upsilon_A^{tilt} E_0^2$ is estimated to be 4.9×10^3 nA/cm, which is 2 orders of magnitude greater than that from the Berry phase effect and the warping effect [38]. To detect the predicted pure AVHC here, one would apply the nonlocal resistance measurement in experiment, which has been widely used for the system without valley polarization [3,5,50,51].

Conclusions. We show that a nonlinear acoustic valley Hall effect emerges in tilted Dirac systems in the complete absence of the warping effect and without considering the Berry phase. It is found that the nonlinear acoustic valley Hall effect has a contribution from the tilting effect and shows a $\sin\theta$ dependence on the orientation of the tilt with respect to the surface acoustic wave. Interestingly, the tilt-induced nonlinear acoustic valley Hall effect shows a relaxation-time independence in the regime $\gamma(E_f, \tau) \gg 1$, which presents an approach to distinguish the contributions from the Berry phase or trigonal warping. We have also calculated the nonlinear acoustic valley Hall effect in the armchair uniaxially strained graphene monolayer with a substrate-induced energy gap. Remarkably, the magnitude of the nonlinear AVHC stemming from the tilt mechanism in the strained graphene is 2 orders larger than those reported arising from the warping effect and the Berry phase in monolayer transition metal dichalcogenides.

Acknowledgments. This work is supported by the National Natural Science Foundation of China (Grants No. 12004107 and No. 12374040), the National Science Foundation of Hunan, China (Grant No. 2023JJ30118), and the Fundamental Research Funds for the Central Universities.

[1] D. Xiao, G.-B. Liu, W. Feng, X. Xu, and W. Yao, Coupled spin and valley physics in monolayers of MoS_2 and other group-VI dichalcogenides, Phys. Rev. Lett. **108**, 196802 (2012).
[2] K. F. Mak, K. L. McGill, J. Park, and P. L. McEuen, The valley Hall effect in MoS_2 transistors, Science **344**, 1489 (2014).
[3] Y. Shimazaki, M. Yamamoto, I. V. Borzenets, K. Watanabe, T. Taniguchi, and S. Tarucha, Generation and detection of pure valley current by electrically induced Berry curvature in bilayer graphene, Nat. Phys. **11**, 1032 (2015).
[4] J. R. Schaibley, H. Yu, G. Clark, P. Rivera, J. S. Ross, K. L. Seyler, W. Yao, and X. Xu, Valleytronics in 2D materials, Nat. Rev. Mater. **1**, 16055 (2016).
[5] Z. Wu, B. T. Zhou, X. Cai, P. Cheung, G.-B. Liu, M. Huang, J. Lin, T. Han, L. An, Y. Wang *et al.*, Intrinsic valley Hall transport in atomically thin MoS_2, Nat. Commun. **10**, 611 (2019).
[6] X.-Q. Yu, Z.-G. Zhu, G. Su, and A.-P. Jauho, Thermally driven pure spin and valley currents via the anomalous Nernst effect

in monolayer group-VI dichalcogenides, Phys. Rev. Lett. **115**, 246601 (2015).
[7] D. Xiao, M.-C. Chang, and Q. Niu, Berry phase effects on electronic properties, Rev. Mod. Phys. **82**, 1959 (2010).
[8] N. Nagaosa, J. Sinova, S. Onoda, A. H. MacDonald, and N. P. Ong, Anomalous Hall effect, Rev. Mod. Phys. **82**, 1539 (2010).
[9] I. Sodemann and L. Fu, Quantum nonlinear Hall effect induced by Berry curvature dipole in time-reversal invariant materials, Phys. Rev. Lett. **115**, 216806 (2015).
[10] T. Low, Y. Jiang, and F. Guinea, Topological currents in black phosphorus with broken inversion symmetry, Phys. Rev. B **92**, 235447 (2015).
[11] Z. Z. Du, C. M. Wang, H.-Z. Lu, and X. C. Xie, Band signatures for strong nonlinear Hall effect in bilayer WTe_2, Phys. Rev. Lett. **121**, 266601 (2018).
[12] Z. Du, C. Wang, S. Li, H.-Z. Lu, and X. Xie, Disorder-induced nonlinear Hall effect with time-reversal symmetry, Nat. Commun. **10**, 3047 (2019).
[13] R. Battilomo, N. Scopigno, and C. Ortix, Berry curvature dipole in strained graphene: A Fermi surface warping effect, Phys. Rev. Lett. **123**, 196403 (2019).
[14] J. I. Facio, D. Efremov, K. Koepernik, J.-S. You, I. Sodemann, and J. van den Brink, Strongly enhanced Berry dipole at topological phase transitions in BiTeI, Phys. Rev. Lett. **121**, 246403 (2018).
[15] Z. Du, C. Wang, H.-P. Sun, H.-Z. Lu, and X. Xie, Quantum theory of the nonlinear Hall effect, Nat. Commun. **12**, 5038 (2021).
[16] A. Bandyopadhyay, N. B. Joseph, and A. Narayan, Non-linear Hall effects: Mechanisms and materials, arXiv:2401.02282.
[17] K. Hamamoto, M. Ezawa, K. W. Kim, T. Morimoto, and N. Nagaosa, Nonlinear spin current generation in noncentrosymmetric spin-orbit coupled systems, Phys. Rev. B **95**, 224430 (2017).
[18] Y. Araki, Strain-induced nonlinear spin Hall effect in topological Dirac semimetal, Sci. Rep. **8**, 15236 (2018).
[19] D.-K. Zhou, Z.-F. Zhang, X.-Q. Yu, Z.-G. Zhu, and G. Su, Fundamental distinction between intrinsic and extrinsic nonlinear thermal Hall effects, Phys. Rev. B **105**, L201103 (2022).
[20] C. Zeng, S. Nandy, and S. Tewari, Fundamental relations for anomalous thermoelectric transport coefficients in the nonlinear regime, Phys. Rev. Res. **2**, 032066(R) (2020).
[21] X.-Q. Yu, Z.-G. Zhu, J.-S. You, T. Low, and G. Su, Topological nonlinear anomalous Nernst effect in strained transition metal dichalcogenides, Phys. Rev. B **99**, 201410(R) (2019).
[22] C. Zeng, S. Nandy, A. Taraphder, and S. Tewari, Nonlinear Nernst effect in bilayer WTe_2, Phys. Rev. B **100**, 245102 (2019).
[23] Y.-L. Wu, G.-H. Zhu, and X.-Q. Yu, Nonlinear anomalous Nernst effect in strained graphene induced by trigonal warping, Phys. Rev. B **104**, 195427 (2021).
[24] R. H. Parmenter, The acousto-electric effect, Phys. Rev. **89**, 990 (1953).
[25] G. Weinreich and H. G. White, Observation of the acoustoelectric effect, Phys. Rev. **106**, 1104 (1957).
[26] A. Wixforth, J. Scriba, M. Wassermeier, J. P. Kotthaus, G. Weimann, and W. Schlapp, Surface acoustic waves on $GaAs/Al_xGa_{1-x}As$ heterostructures, Phys. Rev. B **40**, 7874 (1989).
[27] R. L. Willett, M. A. Paalanen, R. R. Ruel, K. W. West, L. N. Pfeiffer, and D. J. Bishop, Anomalous sound propagation at $\nu = 1/2$ in a 2D electron gas: Observation of a spontaneously broken translational symmetry? Phys. Rev. Lett. **65**, 112 (1990).
[28] V. I. Fal'ko, S. V. Meshkov, and S. V. Iordanskii, Acoustoelectric drag effect in the two-dimensional electron gas at strong magnetic field, Phys. Rev. B **47**, 9910 (1993).
[29] A. Hernández-Mínguez, Y.-T. Liou, and P. V. Santos, Interaction of surface acoustic waves with electronic excitations in graphene, J. Phys. D: Appl. Phys. **51**, 383001 (2018).
[30] P. Delsing, A. N. Cleland, M. J. A. Schuetz, J. Knörzer, G. Giedke *et al.*, The 2019 surface acoustic waves roadmap, J. Phys. D: Appl. Phys. **52**, 353001 (2019).
[31] S. H. Zhang and W. Xu, Absorption of surface acoustic waves by graphene, AIP Adv. **1**, 022146 (2011).
[32] V. Miseikis, J. E. Cunningham, K. Saeed, R. O'Rorke, and A. G. Davies, Acoustically induced current flow in graphene, Appl. Phys. Lett. **100**, 133105 (2012).
[33] V. Parente, A. Tagliacozzo, F. von Oppen, and F. Guinea, Electron-phonon interaction on the surface of a three-dimensional topological insulator, Phys. Rev. B **88**, 075432 (2013).
[34] V. M. Kovalev and A. V. Chaplik, Effect of exciton dragging by a surface acoustic wave, JETP Lett. **101**, 177 (2015).
[35] P. O. Sukhachov and H. Rostami, Acoustogalvanic effect in Dirac and Weyl semimetals, Phys. Rev. Lett. **124**, 126602 (2020).
[36] P. Bhalla, G. Vignale, and H. Rostami, Pseudogauge field driven acoustoelectric current in two-dimensional hexagonal Dirac materials, Phys. Rev. B **105**, 125407 (2022).
[37] P. Zhao, C. H. Sharma, R. Liang, C. Glasenapp, L. Mourokh, V. M. Kovalev, P. Huber, M. Prada, L. Tiemann, and R. H. Blick, Acoustically induced giant synthetic Hall voltages in graphene, Phys. Rev. Lett. **128**, 256601 (2022).
[38] A. V. Kalameitsev, V. M. Kovalev, and I. G. Savenko, Valley acoustoelectric effect, Phys. Rev. Lett. **122**, 256801 (2019).
[39] K. Sonowal, A. V. Kalameitsev, V. M. Kovalev, and I. G. Savenko, Acoustoelectric effect in two-dimensional Dirac materials exposed to Rayleigh surface acoustic waves, Phys. Rev. B **102**, 235405 (2020).
[40] See Supplemental Material at http://link.aps.org/supplemental/10.1103/PhysRevB.109.L161101 for the derivation of equations in the text.
[41] J. C. W. Song, A. V. Shytov, and L. S. Levitov, Electron interactions and gap opening in graphene superlattices, Phys. Rev. Lett. **111**, 266801 (2013).
[42] Y. Fan, M. Zhao, Z. Wang, X. Zhang, and H. Zhang, Tunable electronic structures of graphene/boron nitride heterobilayers, Appl. Phys. Lett. **98**, 083103 (2011).
[43] M. O. Goerbig, Electronic properties of graphene in a strong magnetic field, Rev. Mod. Phys. **83**, 1193 (2011).
[44] S. Haddad and L. Mandhour, Kohn anomaly of optical zone boundary phonons in uniaxial strained graphene: Role of the Dirac cone electronic dispersion, Phys. Rev. B **98**, 115420 (2018).
[45] K. Das, K. Ghorai, D. Culcer, and A. Agarwal, Nonlinear valley Hall effect, arXiv:2307.12088.

[46] G. Giovannetti, P. A. Khomyakov, G. Brocks, P. J. Kelly, and J. van den Brink, Substrate-induced band gap in graphene on hexagonal boron nitride: *Ab initio* density functional calculations, Phys. Rev. B **76**, 073103 (2007).

[47] B. Hunt, J. D. Sanchez-Yamagishi, A. F. Young, M. Yankowitz, B. J. LeRoy, K. Watanabe, T. Taniguchi, P. Moon, M. Koshino, P. Jarillo-Herrero *et al.*, Massive Dirac fermions and Hofstadter butterfly in a van der Waals heterostructure, Science **340**, 1427 (2013).

[48] P. Zomer, S. Dash, N. Tombros, and B. Van Wees, A transfer technique for high mobility graphene devices on commercially available hexagonal boron nitride, Appl. Phys. Lett. **99**, 232104 (2011).

[49] I. G. Savenko, A. V. Kalameitsev, L. G. Mourokh, and V. M. Kovalev, Acoustomagnetoelectric effect in two-dimensional materials: Geometric resonances and Weiss oscillations, Phys. Rev. B **102**, 045407 (2020).

[50] R. Gorbachev, J. Song, G. Yu, A. Kretinin, F. Withers, Y. Cao, A. Mishchenko, I. Grigorieva, K. S. Novoselov, L. Levitov *et al.*, Detecting topological currents in graphene superlattices, Science **346**, 448 (2014).

[51] M. Sui, G. Chen, L. Ma, W.-Y. Shan, D. Tian, K. Watanabe, T. Taniguchi, X. Jin, W. Yao, D. Xiao *et al.*, Gate-tunable topological valley transport in bilayer graphene, Nat. Phys. **11**, 1027 (2015).